

A New Highly Selective Fluorescent Silver Probe

Fangfang Dang · Kewei Lei · Weisheng Liu

Received: 17 May 2007 / Accepted: 4 September 2007 / Published online: 6 November 2007
© Springer Science + Business Media, LLC 2007

Abstract We have synthesized 3,3,7,7-tetra[*N*-ethyl-*N*-benzyl(acetamide)-2-oxymethyl]-5-oxanonane (EBAOO) and its terbium complex. The crystal structures of the complex were determined: [Tb(EBAOO)]₂[Tb(NO₃)₅]₃·H₂O, Orthorhombic, *a*=40.722 (6) Å, *b*=18.418 (3) Å, *c*=20.496 (3) Å. In the structure, the rare earth ion satisfies nine coordination. The geometry of the nine-coordinate polyhedron is discussed in terms of the dihedral angle and the mean plane. The luminescence of the complex is noticeably enhanced upon complexation with Ag⁺, which is due to the suppression of photoinduced electron transfer (PET) process. Therefore, the terbium complex can be used as a selective fluorescent silver probe.

Keywords 3, 3, 7, 7-Tetra[*N*-ethyl-*N*-benzyl(acetamide)-2-oxymethyl]-5-oxanonane · Silver · Terbium · Fluorescent probe

Introduction

Metal ions such as Na⁺, K⁺, Ca²⁺, Zn²⁺ and Ag⁺ play an important role in biological processes. However, investiga-

tion of their function in biological systems can be challenging because these metal ions lack intense visible absorption and emission for easy detection. Chemosensors for these ions provide an approach to such investigation and have received considerable attention [1]. A number of “chromophore–spacer–receptor” systems that can selectively recognize specific guest ions at their receptor site and produce measurable color and/or luminescence changes have been described [2–8]. However, the performance accuracy of these sensors is still limited, and there needs to be improved specific response, in particular, in recognition selectivity for Ag⁺ over other metal ions [9]. This issue necessitates the development of sensor molecules that can adequately discriminate Ag⁺ from other metal ions.

In this endeavor, we have designed a series of multifunctional ligands having both selective ability to coordinate transition metal ions and good luminescence properties with lanthanide ions, considering the unique luminescence properties of rare earth complexes, including hypersensitivity to the coordination environment, narrow bandwidth and millisecond lifetime [10].

In this paper, we report a new chemosensor, the terbium (III) nitrate complexes with 3,3,7,7-tetra[*N*-ethyl-*N*-benzyl(acetamide)-2-oxymethyl]-5-oxanonane (EBAOO; Fig. 1), which can signal Ag⁺ specifically. The nitrogen atoms in this ligand serve as silver ion receptor. In the absence of cations, the emission of the complex is partially quenched by photoinduced electron transfer (PET) from nitrogen lone pairs. However, upon complexation of a metal ion, binding the nitrogen lone pair electrons by the metal ion complexation partially suppresses the PET process. For complexation with Ag⁺, the luminescence is noticeably enhanced. Thus, the complex can be utilized as a chemosensor specific for detection of Ag⁺ by monitoring the changes in luminescence.

F. Dang · K. Lei · W. Liu (✉)
Department of Chemistry and State Key Laboratory of Applied Organic Chemistry, College of Chemistry and Chemical Engineering, Lanzhou University, Lanzhou 730000, People's Republic of China
e-mail: liuws@lzu.edu.cn

F. Dang
School of Science,
Xi'an University of Architecture & Technology,
Xi'an 710055, People's Republic of China

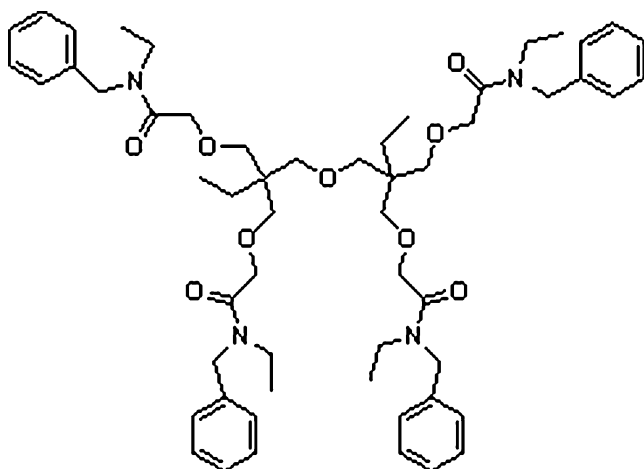


Fig. 1 Structure of 3,3,7,7-tetra[*N*-ethyl-*N*-benzyl(acetamide)-2-oxymethyl]-5-oxanonane (EBAOO)

Experimental section

Reagents

All commercially available chemicals were of A.R. grade and all solvents used were purified by standard methods.

Apparatus

Elemental analyses were determined on an Elementar Vario EL analyzer. IR-spectra were measured on Nicolet Nexus 670 FT-IR using KBr pellets in the range of 400–4,000 cm^{-1} . The ^1H NMR spectra were recorded on a Varian 300 spectrometer using CDCl_3 as solvent and TMS as external reference. Fluorescence measurements were performed on a Hitachi F-4500 spectrophotometer equipped with quartz cuvettes of 1 cm path length. The excitation and emission slit widths were 10 nm. Intensity data were collected at room temperature on a Bruker SMART CCD area-detector diffractometer using graphite monochromated $\text{MoK}\alpha$ radiation. The semi-empirical absorption correction (multi-scan) was applied. The structures of the titled compounds were solved by applying the direct method using a Bruker SHELXTL and refined by a full-matrix least-squares refinement on F^2 using SHELEX 97. The non-H atoms were refined with anisotropic displacement parameters.

Preparation of EBAOO and the terbium complex

A solution of 3,3,7,7-tetrahydroxymethyl-5-oxanonane (2.5 g, 10 mmol) in THF was added dropwise into a THF solution that was suspended with NaH (1.6 g, 60%, 40 mmol), and the mixture was stirred under nitrogen at room temperature until no gas appeared. Then a solution of *N*-ethyl-*N*-benzylchloroacetamide (8.7 g, 44 mmol) in THF was added

dropwise into the mixture. After the mixture was refluxed for 6 h, the THF was evaporated and the residue was washed by column chromatography (silica gel, 2:1 $\text{CHCl}_3/\text{CH}_3\text{CO}_2\text{Et}$) and evaporated in vacuum resulted a yellow oil (4.3 g), yield, 50%. Anal. Calcd. for $\text{C}_{56}\text{H}_{78}\text{N}_4\text{O}_9$ (%): C, 70.71; H, 8.26; N, 5.89. Found: C, 70.65; H, 8.31; N, 5.85. ^1H NMR (300 MHz, CDCl_3) δ 0.81 (6H), 1.05 (12H), 1.10 (4H), 3.22–3.36 (20H), 4.04–4.17 (8H), 4.53–4.57 (8H), 7.18–7.32 (20H) ppm.

The terbium (III) complex was also synthesized. An ethyl acetate solution of $\text{Tb}(\text{NO}_3)_3 \cdot 6\text{H}_2\text{O}$ (0.25 mmol) was added dropwise to a solution of the ligand (0.1 mmol) in the ethyl acetate (20 ml). The mixture was stirred for 4 h and white precipitate formed. The precipitate was collected and washed three times with ethyl acetate. Further drying in vacuum afforded a powder, yield, 75–80%. The single crystal was grown from acetone with slow evaporation at room temperature. About 1 week later, transparent crystals formed from the solution.

Results and discussion

IR spectra

The IR spectrum of EBAOO shows bands at 1,637 and 1,044 cm^{-1} , which may be assigned to $\nu(\text{C}=\text{O})$, $\nu(\text{C}-\text{O}-\text{C})$ respectively. In the IR spectra of the complexes, these bands shift by about 23 cm^{-1} , and 14 cm^{-1} toward lower wavenumbers, thus indicating that the $\text{C}=\text{O}$, ether O atoms take part in coordination to the metal ion. The absorption bands assigned to the coordinated nitrates were observed at 1,497 and 1,311 cm^{-1} for the complex. It indicates that coordinated nitrate groups in the complex are bidentate and there is no free nitrate [11], which is demonstrated by the crystal structures illuminated as follows.

Determination of the X-ray structure

The crystal data and refinement results of the complex are summarized in Table 1. Selected bond lengths and angles are given in Table 2. Figure 2a shows the structure and the atomic numbering schemes. As we can see from Fig. 2a, four chains of EBAOO stretch around and form a cup-like cavity to encapsulate the metal ion, the nine oxygen atoms of EBAOO all take part in the coordination, the nitrogen atoms of the four chains do not coordinate. Five nitrates chelate a Tb^{3+} to form the big counter anion, and one H_2O lies outside of the coordination sphere. For the nine oxygen atoms coordinated to Tb1, the five ether oxygen atoms appear to be all at the same distance, $2.47 \pm 0.05 \text{ \AA}$, and the other four Tb1-carboxylate oxygen bond distances are slighter shorter, and

Table 1 Crystal and experimental data

Characteristic	
Empirical formula	C ₁₁₂ H ₁₅₈ N ₂₃ O ₆₄ Tb ₅
Formula weight	3645.21
Wavelength	0.71073 Å
Temperature	298 (2) K
Crystal system	Orthorhombic
Space group: <i>Pbcn</i>	Z=4
<i>a</i>	40.722(6) Å
<i>b</i>	18.418(3) Å
<i>c</i>	20.496(3) Å
<i>V</i>	15372(4) Å ³
<i>D_x</i>	1.575 g/cm ³
Absorption coefficient	2.366 mm ⁻¹
<i>F</i> (000)	7,312
Crystal size	0.42×0.39×0.37 mm
θ range	2.22 to 25.01°
Limiting indices	-47<= <i>h</i> <=48, -21<= <i>k</i> <=16, -24<= <i>l</i> <=23
Reflections collected/ unique	77,078/13,413 [<i>R</i> (int)=0.1105]
Completeness (to θ =25.01°)	99.0%
Absorption correction	Semi-empirical from equivalents
Max. and min. transmission	0.4748 and 0.4365
Goodness of fit on <i>F</i> ²	1.058
Final <i>R</i> indices [<i>I</i> >2σ(<i>I</i>)]	<i>R</i> 1=0.0753, <i>wR</i> 2=0.1710
<i>R</i> indices (all data)	<i>R</i> 1=0.1684, <i>wR</i> 2=0.2371
Largest diff. peak and hole	1.417 and -2.103 eÅ ⁻³
Measurement	Bruker SMART CCD area-detector diffractometer
Program system	SHELXL-97
Structure determination	Direct method
Refinement	Full matrix

CCDC 284126 contains the supplementary crystallographic data for this paper. These data can be obtained free of charge from The Cambridge Crystallographic, Data Centre via www.ccdc.cam.ac.uk/data_request/cif.

lie in the range of 2.30–2.39 Å. In the crystal structure, it is notable that the ratio of Tb to EBAOO is 5:2, but cation/anion is 2:3, which is rare in rare earth complexes.

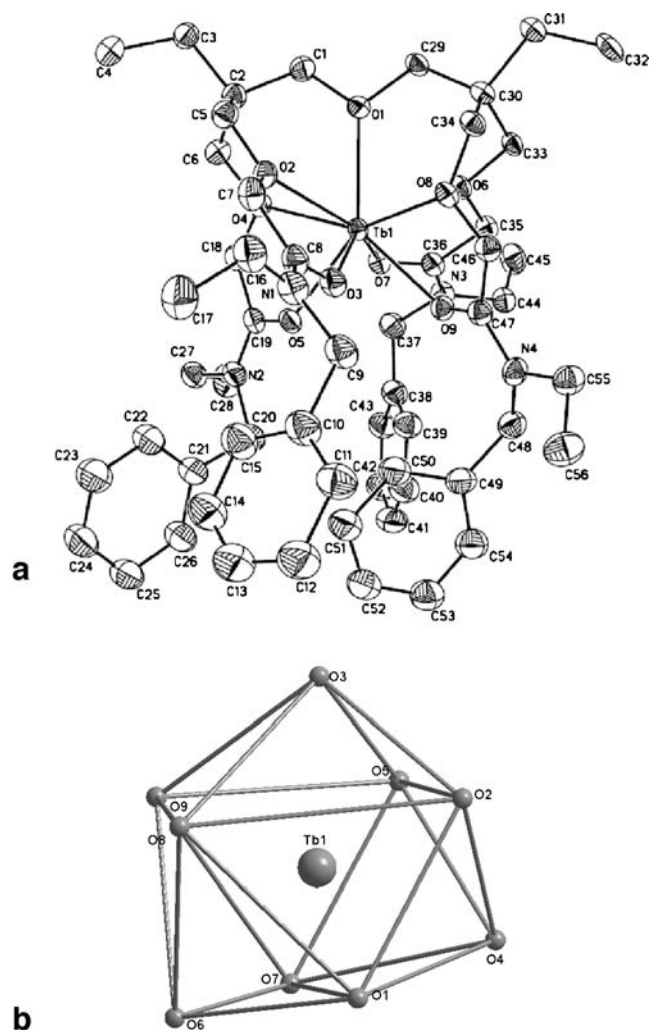
Nine-coordinated Ln (III) complexes most frequently form tricapped trigonal prism (TCTP) or capped square antiprism (CSAP) polyhedrons. As shown in Fig. 2b, the TCTP geometry can be accessed using the three rectangular (O2–O5–O9–O8, O2–O5–O7–O1, O8–O9–O7–O1) and two triangular (O2–O8–O1, O5–O9–O7) faces of the trigonal prism and the three atoms occupying the capping positions (O3, O4, O6). The dihedral angles (δ) between pairs of adjacent triangular faces, O3(O2O5)O4, O4(O1O7)O6 and O6(O8O9)O3, were calculated to be 21.10, 5.54 and 50.18°, respectively. Significant deviation from the ideal TCTP geometry in the range of 15–45°, can be found in the

5.54° of O4(O1O7)O6. This dihedral angle suggests that O4, O1, O7 and O6 are almost planar. The mean standard deviation of the four atoms in this plane is 0.0979. The O4 and O6 atoms are located 0.044 and 0.053 Å above the

Table 2 The selected bond lengths (Å) and angles (°) for Tb(EBAOO)₂[Tb(NO₃)₅]₃·H₂O

Bond lengths (Å) and angles (°)	
Tb1–O9	2.295 (9)
Tb1–O5	2.328 (9)
Tb1–O3	2.384 (10)
Tb1–O7	2.391 (9)
Tb1–O4	2.421 (9)
Tb1–O8	2.428 (9)
Tb1–O1	2.435 (9)
Tb1–O2	2.511 (9)
Tb1–O6	2.525 (8)
O(9)–Tb(1)–O(5)	85.0 (3)
O(9)–Tb(1)–O(3)	73.8 (3)
O(5)–Tb(1)–O(3)	73.7 (4)
O(9)–Tb(1)–O(7)	79.6 (3)
O(5)–Tb(1)–O(7)	72.9 (3)
O(3)–Tb(1)–O(7)	138.6 (4)
O(9)–Tb(1)–O(4)	144.4 (3)
O(5)–Tb(1)–O(4)	65.5 (3)
O(3)–Tb(1)–O(4)	113.4 (3)
O(7)–Tb(1)–O(4)	73.2 (3)
O(9)–Tb(1)–O(8)	65.2 (3)
O(5)–Tb(1)–O(8)	138.0 (3)
O(3)–Tb(1)–O(8)	70.0 (3)
O(7)–Tb(1)–O(8)	125.3 (3)
O(4)–Tb(1)–O(8)	150.3 (3)
O(9)–Tb(1)–O(1)	132.9 (3)
O(5)–Tb(1)–O(1)	141.3 (3)
O(3)–Tb(1)–O(1)	118.5 (3)
O(7)–Tb(1)–O(1)	102.9 (3)
O(4)–Tb(1)–O(1)	76.4 (3)
O(8)–Tb(1)–O(1)	76.6 (3)
O(9)–Tb(1)–O(2)	134.6 (3)
O(5)–Tb(1)–O(2)	91.7 (3)
O(3)–Tb(1)–O(2)	61.9 (3)
O(7)–Tb(1)–O(2)	142.2 (3)
O(4)–Tb(1)–O(2)	69.0 (3)
O(8)–Tb(1)–O(2)	89.4 (3)
O(1)–Tb(1)–O(2)	67.7 (3)
O(9)–Tb(1)–O(6)	72.7 (3)
O(5)–Tb(1)–O(6)	131.7 (3)
O(3)–Tb(1)–O(6)	134.6 (3)
O(7)–Tb(1)–O(6)	61.4 (3)
O(4)–Tb(1)–O(6)	111.7 (3)
O(8)–Tb(1)–O(6)	68.7 (3)
O(1)–Tb(1)–O(6)	68.3 (3)
O(2)–Tb(1)–O(6)	134.2 (3)
O(7)–Tb(1)–O(1)	102.9 (3)
O(4)–Tb(1)–O(1)	76.4 (3)
O(8)–Tb(1)–O(1)	76.6 (3)

Fig. 2 View of the [Tb(EBAOO)]₂[Tb(NO₃)₅]₃·H₂O showing atom labeling and ellipsoids at 30% (a) and the arrangement of the atoms for the polyhedrons (b). In this view, hydrogen atoms are omitted for clarity



mean plane, respectively, while the O1 and O7 atoms are displaced in the opposite direction by 0.045 and 0.053 Å, respectively. The mean standard deviation of the plane formed by O2, O5, O9 and O8 is 0.1024. The O2 and O9 atoms are located 0.040 and 0.061 Å above the mean plane, respectively, while the O5 and O8 atoms are displaced in the opposite direction by 0.045 and 0.056 Å, respectively. In CSAP, the Tb (III) ion is located 0.840 Å below the upper plane (O2–O5–O9–O8) and 1.431 Å above the lower plane (O4–O7–O6–O1). The displacement of each atom from the mean plane shows that the Tb (III) complex forms a slightly distorted capped square polyhedron.

Fluorescence spectroscopy

The luminescence response of the complex to Ag⁺ is unique. Significant changes in emission intensities of the fluorescent spectra occurred upon the addition of minute amounts of Ag⁺ ions (Fig. 3). As mentioned above, the four nitrogen atoms of EBAOO did not coordinate with Tb³⁺. The emission of the complex in methanol (1 × 10^{−4} M), when excited

at 320 nm, is partially quenched by photoinduced electron transfer (PET) from nitrogen lone pairs. Upon addition of a methanolic silver ion solution, the fluorescent spectra of

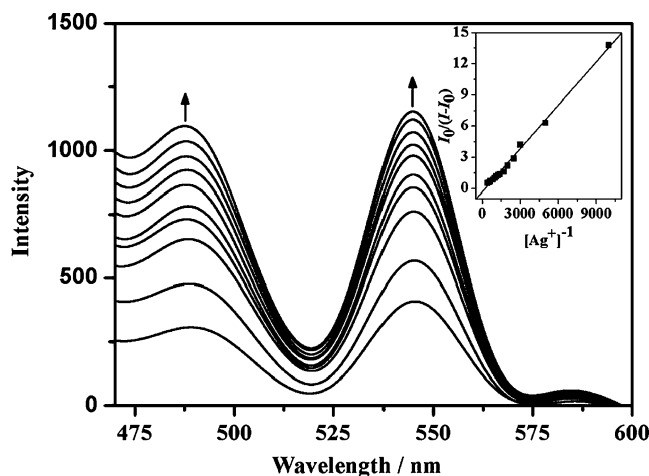


Fig. 3 Fluorescence spectra of Tb-EBAOO (1 × 10^{−4} M) in methanol in the presence of Ag⁺. The *insert* shows the plot of $I_0/(I-I_0)$ vs $[Ag^+]^{-1}$. Excitation was at 320 nm

the complex showed a noticeable enhancement in emission which often accompanies the complexation [12]. After addition of silver ion, binding the nitrogen lone pair electrons by metal ion complexation partially suppresses the PET process, causing the fluorescence to increase [13, 14].

The insert in Fig. 3 shows the plot of $I_0/(I-I_0)$ versus $[\text{Ag}^+]^{-1}$, where I_0 and I represent the emission intensity at 546 nm in the absence and presence of Ag^+ , respectively. The yielded straight line further confirms that the complexation of Ag^+ is in a 1:1 ratio. The 1:1 complexation constant can be calculated from the emission intensity and the concentration of metal ion, $[\text{M}]$, as follows [14, 15]:

$$\frac{I - I_0}{I_\infty - I} = K \left\{ [\text{M}]_t - [\text{L}]_t \left(\frac{I - I_0}{I_\infty - I_0} \right) \right\}$$

where I_∞ is the emission response when no further change occurred upon continued addition of silver ions. $[\text{L}]_t$ is the total concentration of the complex molecule and $[\text{M}]_t$ represents the total silver ion concentration. The complexation constant is 1,037 L/mol, which is calculated using a non-linear curve-fitting method [16] with the observed experimental emission.

It is of particular interest that the addition of other metal ions such as Na^+ , K^+ , Ca^{2+} , Ba^{2+} , and Zn^{2+} , etc., in the same concentration reveal no increase or a faint response to the fluorescent intensity of the complex, despite complexation with the nitrogen atom as reflected in the absorption spectrum changes. Evidently, the complex can remarkably discriminate Ag^+ from other metal ions.

Conclusion

The ligand, 3,3,7,7-tetra[*N*-ethyl-*N*-benzyl(acetamide)-2-oxymethyl]-5-oxanonane (EBAOO) and its terbium complex were synthesized. The crystal structures of the complex were determined: $[\text{Tb}(\text{EBAOO})_2[\text{Tb}(\text{NO}_3)_5]_3 \cdot \text{H}_2\text{O}]$. The geometry of the nine-coordinate polyhedron is discussed in terms of the dihedral angle and the mean plane. The luminescence of the complex is noticeably enhanced upon complexation with Ag^+ , which is due to the suppression of photoinduced electron transfer (PET) process. In contrast, the addition of other metal ions such as Na^+ , K^+ , Ca^{2+} , Ba^{2+} , and Zn^{2+} , etc., in the same concentration reveal no increase or a faint response to the fluorescent intensity of the complex, despite

complexation with EBAOO. Therefore, the terbium complex can be used as a selective fluorescent silver probe.

Acknowledgements We are grateful to the NSFC (20431010, 20621091 and J0630962) for financial support.

References

1. Wason WT (1993) Fluorescence and luminescence probes for biological activity. Academic, San Diego, CA
2. Czarnik AW (1993) Fluorescent chemosensors for ion and molecule recognition. American Chemical Society, Washington, DC
3. Burdette SC, Lippard SJ (2001) ICC34-golden edition of coordination chemistry reviews. Coordination chemistry for the neurosciences. Coord Chem Rev 216–217:333–361
4. de Silva AP, Gunaratne HQ, Gunnlaugsson T, Huxley AJM, McCoy CP, Rademacher JT, Rice TE (1997) Signaling recognition events with fluorescent sensors and switches. Chem Rev 97:1515–1566
5. Amendola V, Fabbrizzi L, Licchelli M, Mangano C, Pallavicini P, Parodi L, Poggi A (1999) Molecular events switched by transition metals. Coord Chem Rev 192:649–669
6. Valeur B, Leray I (2000) Design principles of fluorescent molecular sensors for cation recognition. Coord Chem Rev 205:3–40
7. Burdette SC, Walkup GK, Spingler B, Tsien RY, Lippard SJ (2001) Fluorescent sensors for Zn^{2+} based on a fluorescein platform: Synthesis, properties and intracellular distribution. J Am Chem Soc 123:7831–7841
8. Chen CT, Huang WP (2002) A highly selective fluorescent chemosensor for lead ions. J Am Chem Soc 124:6246–6247
9. Su CC, Liu LK, Lu LH (2006) Sensing and fluorescence behaviors of complex formation between new lariat crown ethers bearing fluorescence sidearm and metal ions in methanol solution. J Lumin 121:159–172
10. Richardson FS (1982) Terbium(III) and europium(III) ions as luminescent probes and stains for biomolecular systems. Chem Rev 82:541–552
11. Nakamoto K (1986) Infrared and Raman spectra of inorganic and coordination compounds, 4th edn. Wiley, New York
12. Liu WS, Jiao TQ, Li YZ, Liu QZ, Tan MY, Wang H, Wang LF (2004) Lanthanide coordination polymers and their Ag^+ -modulated fluorescence. J Am Chem Soc 126:2280–2281
13. Ji HF, Brown GB, Dabestani R (1999) Calix[4]arene-based Cs^+ selective optical sensor. Chem Commun 609–610
14. de Silva AP, Sandanayake KRAS (1989) Fluorescent PET (photo-induced electron transfer) sensors for alkali metal ions with improved selectivity against protons and with predictable binding constants. J Chem Soc Chem Commun 1183–1184
15. Ji HF, Dabestani R, Brown GM, Sachleben RA (2000) A new highly selective calix[4]crown-6 fluorescent caesium probe. Chem Commun 833–834
16. Ji HF, Dabestani R, Brown GM, Hettich RL (1999) Spacer Length Effect on the PET Fluorescent Probe for Alkali Metal Ions. Photochem Photobiol 69:513–516